Ocean Sci. Discuss., 5, 281–325, 2008
www.ocean-sci-discuss.net/5/281/2008/

Ocean Science Discussions

Papers published in *Ocean Science Discussions* are under open-access review for the journal *Ocean Science*

Geothermal heating, diapycnal mixing and the abyssal circulation

J. Emile-Geay[1,*] **and G. Madec**[2,**]

[1]Département Terre-Atmosphère-Océan, Ecole Normale Supérieure, Paris, France
[2]Laboratoire d'Océanographie et du Climat: Expérimentations et Approches Numériques, Unité Mixte de Recherche 7159 CNRS/IRD/UPMC/MNHN, Institut Pierre Simon Laplace, Paris, France
[*]now at: Dept. of Earth and Atmospheric Sciences, Georgia Inst. of Technology, Atlanta, USA
[**]also at: National Oceanography Centre, Southampton, UK

Received: 21 May 2008 – Accepted: 26 May 2008 – Published: 7 July 2008

Correspondence to: J. Emile-Geay (julien@gatech.edu)

Published by Copernicus Publications on behalf of the European Geosciences Union.

Abstract

The dynamical role of geothermal heating in abyssal circulation is reconsidered using three independent methods.

First, we show that a uniform geothermal heat flux close to the observed average (86.4 mW m^{-2}) supplies as much heat to the abyss as diapycnal mixing with a rate of ~1 cm^2 s^{-1}. A simple scaling law, based upon a purely advective balance, indicates that such a heat flux is able to generate a deep circulation of order 5 Sv (1 Sv≡10^6 m^{3}s^{-1}) associated with the Antarctic Bottom Water mass (AABW). Its intensity is inversely proportional to the strength of deep temperature gradients.

Second, this order of magnitude is confirmed by the density-binning method (Walin, 1982) applied to the observed thermohaline structure of Levitus (1998). Additionally, the method allows to investigate the effect of realistic spatial variations of the flux obtained from heatflow measurements and classical theories of lithospheric cooling. It is found that a uniform heatflow forces a transformation of about 6 SV at σ_4=45.90, consistent with the previous estimate. The result is very similar for a realistic heatflow, albeit shifted towards slightly lighter density classes.

Third, we use a general ocean circulation model in global configuration to perform three sets of experiments: (1) a thermally homogenous abyssal ocean with and without uniform geothermal heating; (2) a more stratified abyssal ocean subject to (i) no geothermal heating, (ii) a constant heat flux of 86.4 mW m^{-2}, (iii) a realistic, spatially varying heat flux of identical global average; (3) experiments (i) and (iii) with enhanced vertical mixing at depth. It is found, for strong vertical mixing rates, that geothermal heating enhances the AABW cell by about 15% (1.5 Sv) and heats up the last 2000 m by 0.3°, reaching a maximum of 0.5° in the deep North Pacific. Its impact is even stronger in a weakly diffusive deep ocean. The spatial distribution of the heat flux acts to enhance this temperature rise at mid-depth and reduce it at great depth, producing a more moderate increase in overturning than in the uniform case.

OSD

5, 281–325, 2008

The three approaches converge to the conclusion that geothermal heating is an important actor of abyssal dynamics, and should no longer be neglected.

1 Introduction

The abyssal circulation is generally pictured as closing the heat budget between downward diffusion from the warm surface layers and a widespread upwelling of cold, deep waters, balancing highly localized deep water sources (Warren, 1981). Stommel and Arons (1960) first explored the consequences of this statement by assuming a uniform upwelling rate at the base of the main thermocline, and showing that this would govern a Sverdrup-like circulation in the interior, from which they inferred the necessary existence of deep western-boundary currents accomplishing interbasin mass transport. The existence and directions of these currents had been suggested by laboratory experiments Stommel, Arons and Faller (1958) and was later confirmed by in situ measurements (see Arhan et al., 1998; Whitworth et al., 1999, and references therein). In this framework, the driving force of the abyssal circulation is the downward diffusion of heat, which controls the global upwelling rate, thereby setting the magnitude of the meridional overturning circulation (MOC). This classical view still prevails in spite of much work having been done to understand the effect of non-uniform mixing rates and wind-forced upwelling in the Southern Ocean (Webb and Suginohara, 2001; Toggweiler and Samuels, 1995, 1998; Visbeck, 2007).

Of course, the deep ocean has another source of heat: geothermal heating due to lithospheric cooling. Yet it is usually neglected from an oceanographic point of view because this flux is less than 2% of surface heat fluxes (Huang, 1999): a total power of 0.03 PW and a mean flux of $\sim$88 mW m^{-2} (Stein and Stein, 1992), while surface fluxes are of order 30 to 250 W m^{-2}. Although it is clear that geothermal heat flux is weak compared to the surface ones, this is not the relevant comparison. First, geothermal heat flux is systematically positive whereas surface fluxes are of both signs, leading to important cancelations on a global scale. Second, the geothermal heat flow acts only

OSD
5, 281–325, 2008

on the densest water masses, which are only in contact with the atmosphere in very limited areas at high latitudes, where they are formed through heat and freshwater loss to the atmosphere and sea-ice. Those deep-water formation areas only represent a few thousandths of the global ocean surface, as opposed to a geothermal heat flux spanning the entire seafloor. It turns out that the ratio between the AABW outcropping area and the total seafloor area is about one to a thousand, and consequently surface integrals of the two fluxes scale comparably.

In the present study, we focus on the large-scale geothermal heat flux – ignoring the localized effect of hydrothermal vents – and ask how it affects the *global* abyssal circulation. A similar question was raised by Adcroft et al. (2001), using an ocean general circulation model (GCM) in global configuration to assess the effect of a uniform heatflow of $50\,\mathrm{mW\,m^{-2}}$ at the base of their model. They obtained a first order change in abyssal water properties (a warming of about 0.3 to 0.5°C) and a fairly weak dynamical response (about 1.8 Sv in the Indo-Pacific). These original results were further clarified by Scott et al. (2001) in an idealized setting. Their essential finding is that the response to geothermal heating is largely advective: a deep circulation cell communicates the anomalous heat to the surface so that steady-state can be achieved. Moreover, they found this circulation to require the existence of a background ("Stommel-Arons") circulation, and to be inversely proportional to the deep stratification. The goal of this article is to further clarify the interaction between geothermal and background circulations, in a more realistic setting. In so doing, we must take into account the spatial variations of the heatflow.

As far as we know, such a dataset does not currently exist, as the measurement of conductive heatflow in the superficial sediments are too sparse. To fill in the blanks, Pollack et al. (1993) proposed to use the age of the bedrock, which is reasonably well known (Müller et al., 1997), as a proxy for heatflow[1]. Like Pollack et al. (1993), we used

[1]We did not follow Huang (1999)'s suggestion to use the bathymetry as a proxy for the age of lithosphere, for this produced unrealistically large fluxes in regions where small-scale topographical structures are present (e.g. coral reefs, continental margins, hot spot tracks,

the Stein and Stein (1992) formula relating the heatflow (in $\mathrm{mW\,m^{-2}}$) to the age of the bedrock, t, in million years (Ma):

$$Q_{\mathrm{geo}} = \begin{cases} 510\, t^{-1/2} & \text{if } t \leq 55 \text{ Ma}, \\ 48 + 96 \exp(-0.027\, t) & \text{if } t > 55 \text{ Ma}\,. \end{cases} \quad (1)$$

The seafloor age was taken from the Müller et al. (1997) high-resolution global dataset ($0.1^\circ \times 0.1^\circ$), containing very few regions of undetermined age. Their surface is quite significant, though, especially East of Australia and Indonesia. In those regions, the flux was prolonged by continuity, in order to preserve the smooth structure obtained elsewhere with this method.

This spatial representation is shown in Fig. 1. One clearly recognizes the ridge system, where oceanic lithosphere is formed at high temperature (about 1350°C), before cooling down and thickening away from the ridge as plates diverge. Ridges therefore display a maximum heat flux, while the minimum is $\sim 50\,\mathrm{mW\,m^{-2}}$ on the deepest (and oldest) abyssal plains. Since Eq. (1) becomes singular for young ages, Q_{geo} was bounded to $400\,\mathrm{mW\,m^{-2}}$, as 95% of measurements fall below this value. This yields a global mean of $86.4\,\mathrm{mW\,m^{-2}}$, compatible with observations (Pollack et al., 1993).

The paper is structured as follows: in Sect. 2 we complete the existing theory for the abyssal circulation, explicitly including the contribution of geothermal heating, and use a simple scaling law to assess the magnitude of the geothermally-induced circulation. We then refine this estimate in Sect. 3, using the thermodynamic method of density-binning, and investigate the effect of the spatial structure of the flux. In Sect. 4, we report the results of 3 sets of experiments carried with an ocean GCM in the presence of (1) no geothermal heating, (2) uniform geothermal heating, (3) spatially variable geothermal heating. Discussion follows in Sect. 5.

ninety-west ridge): the latter are largely uncorrelated with the planetary-scale structures due to thermal subsidence.

2 A simple theory for the abyssal circulation

2.1 Geothermal vs diapycnal fluxes

Let us consider the heat budget of a volume of seawater in contact with the seafloor, with unit horizontal surface and height h. The heat per unit mass is $C_p T$ and its conservation equation writes:

$$\partial_t T + \mathbf{u}\cdot\boldsymbol{\nabla} T = \boldsymbol{\nabla}\cdot(K\boldsymbol{\nabla} T) + \frac{Q_{\text{geo}}}{\rho_\circ C_p}\delta(z+H) \tag{2}$$

where T is the *potential* temperature, K is the thermal diffusivity, $\rho_\circ$ a reference density (namely $1025\,\text{kg}\,\text{m}^{-3}$), Q_{geo} the geothermal heat flux (about $86.4\,\text{mW}\,\text{m}^{-2}$ on a global average) and C_p the heat capacity of seawater. The delta-function means that the flux is only present at the bottom, $z=-H(x,y)$, and vanishes in the interior (for dimensional consistency, the δ function embodies the dimension of an inverse length). Equivalently, it is the bottom boundary condition of the interior diffusive heat flux, i.e.:

$$\rho_\circ C_p K_z \partial_z T \Big|_{z=-H} = Q_{\text{geo}}(x,y) \tag{3}$$

Geothermal heat flux must be compared to the relevant quantity for abyssal dynamics: the downward, turbulent heat flux, which is thought to control abyssal circulation. This flux is the product of the vertical thermal gradient by the vertical mixing coefficient (K_z). The former can be estimated from the Levitus (1998) temperature data, knowing that their resolution at depth is of order 200 m, up to 500 m below 3750 m. The latter is very poorly known. As *Munk and Wunsch* (1998) pointed out, the deep ocean suffers a "dichotomy of diffusivities", since the value inferred by Munk (1966) to sustain abyssal stratification against global upwelling associated with 25 Sv of deep water formation is

OSD
5, 281–325, 2008

about $10^{-4}\,m^2\,s^{-1}$, which contrasts sharply with the $10^{-5}\,m^2\,s^{-1}$ given by microstructure (Gregg, 1989; Kunze and Sanford, 1996) and dye release measurements (Ledwell et al., 1998) away from regions of rough topography. One way to compare the upward geothermal flux and the downward diffusive flux is to consider a fixed diapycnal mixing coefficient of, say, $10^{-4}\,m^2\,s^{-1}$ and then compute an upper bound for the downward diffusive flux using the temperature data. This is done in Fig. 2: near the bottom, it is clear that even for such a strong mixing rate, geothermal heating O($100\,mW\,m^{-2}$) is directly comparable to turbulent mixing.

Another way to see this is to use the same temperature data to determine the vertical gradient, and to diagnose the value that K_z would need take for the diffusive heat flux to be as great as a geothermal heating of $86.4\,mW\,m^{-2}$. Note that this is not a balance per se, since both fluxes bring heat into the abyss, but is a simple way of comparing their relative magnitudes.

This "equivalent K_z" is defined by the relation:

$$|K_z| = \left| \frac{Q_{geo}}{\rho_\circ C_p} \right| \left| \frac{\partial T}{\partial z} \right|^{-1} \tag{4}$$

which is plotted in Fig. 3 for $z=-4000\,m$. It appears that this diagnosis requires, over much of the ocean, $K_z \geq 1\,cm^2\,s^{-1}$ (this is especially true in the North Pacific, where deep stratification is very weak). In the Western Boundary regions of the southern Hemisphere, such as the Brazil basin, the superposition of the relatively warm North Atlantic Deep Water (NADW) over the cold Antarctic Bottom Water (AABW) is responsible for a very strong vertical temperature gradient. As a result, even small mixing can produce a downward heat flux as strong as geothermal heating. We therefore expect geothermal heat flux to be dynamically important in the North Pacific, but insignificant in the Brazil basin. Averaging on the global scale, we obtain that a geothermal heating of $86.4\,mW\,m^{-2}$ is equivalent to a mean diapycnal mixing rate of $1\,cm^2\,s^{-1}$. We are thus brought to the conclusion that geothermal heating is a major forcing term of the

thermal balance of abyssal water, not at all negligible compared to diapycnal mixing. This must have important dynamic implications.

2.2 A simple scaling law for the geothermally-induced circulation

Since the work of Stommel and Arons (1960) and the clear demonstration of Bryan (1987), it is thought that the intensity of abyssal circulation is chiefly controlled by the heat supplied to the deep ocean. While NADW is now understood to be a largely adiabatic circulation mainly driven by surface forcing and mixing in the Southern Ocean (Toggweiler and Samuels, 1995, 1998; Webb and Suginohara, 2001; Iudicone et al., 2008a,b), the circulation associated with AABW shows great sensitivity to vertical mixing parameterization in most ocean general circulation models (as will be seen again in Sect. 4).

In steady-state, the heat supplied by downward diffusive heat flux convergence must be compensated by advection of colder water in order to close the budget. In other words, a circulation must develop to connect sources and sinks. The heat brought down by vertical mixing can be compensated by an upwelling of cold, deep water. For geothermal heating, which heats up bottom water, the only possible cold source is lateral advection. What is the magnitude of such a circulation ?

Consider the steady state heat Eq. (2). For a fixed thermohaline structure, it is linear in the forcing (diffusion+geothermal heatflow), hence for small velocities we are solving a linear equation, splitting the velocity field into a diffusively-forced and a geothermally-forced component. In the absence of mixing, the input of heat through the seafloor must be balanced by the advection of cold water coming from high southern latitudes (AABW). Let us quantify this advection on a bow-shaped trajectory between a vertical section at, say, 45° S and a horizontal section at 3500 m, which is the core of the AABW cell (cf. Fig. 4).

The balance writes:

$$\mathbf{u} \cdot \boldsymbol{\nabla} T = \frac{Q_{\text{geo}}}{\rho_\circ C_p} \delta(z + H) \tag{5}$$

We add the hypothesis that every lagrangian particle undergoes the same temperature difference ΔT along the way (i.e. the input and output temperature differences between the two sections are constant). As we shall see, this greatly helps understanding the essential physics and can be relaxed easily. Integrating over the volume of the box (cf. Fig. 4), we get an expression for the transport S:

$$S = \frac{Q_{\text{geo}} \mathcal{A}}{\rho_\circ C_p \Delta T} \propto \frac{Q_{\text{geo}}}{\Delta T} \tag{6}$$

where $\mathcal{A}$ is the seafloor area of integration. ΔT can be estimated using the Levitus temperature data. The results of this computation by sub-basins are given in Table 1, where it can be seen that the circulation implied is on the order of several Sverdrups (i.e. commensurate with that generated by diapycnal mixing).

The main result is that the transport is proportional to the heat input Q_{geo}, and inversely proportional to the temperature difference ΔT (as remarked by Scott et al., 2001): an intense circulation will not allow AABW to warm up very much on its northward journey along the bottom; a more sluggish one will imply a greater temperature difference along the way. It should be borne in mind, however, that the thermal structure upon which geothermal heat flux is acting is primarily determined by diapycnal mixing. The latter acts to map surface temperature gradients onto the bottom: the stronger its is, the warmer the temperature at 3500 m, the larger ΔT, and the weaker the geothermal component of the circulation. Note that as long as mixing is not entirely absent (as in nature), $\Delta T \neq 0$, and geothermal transport is well-defined. One should also be cognizant of the fact that this linear decomposition will break down as the density field adjusts to both diffusion and geothermal heating, an effect that will be assessed with a numerical model in Sect. 4.

Thus, this simple calculation suggests that the geothermally-induced circulation is far from negligible, and in fact commensurable to the Stommel-Arons circulation. This contradicts the common opinion, and in particular a previous study by Joyce et al. (1986). The next section aims at reconciling these seemingly opposite views.

2.3 What happens to the Sverdrup balance?

The geothermally-induced circulation should not escape the requirements of vorticity balance. Intrigued by the unambiguous signature of geothermal heating found in the deep North Pacific temperature field (Gordon and Gerard, 1970), Joyce et al. (1986) assessed its effect on the vorticity field. They suggested that geothermal heat flux had a negligible dynamical impact, which is challenged by the results of Scott et al. (2001) and ours. We wish to revisit the argument of Joyce et al. (1986) by retracing their reasoning.

In their formulation, small-scale vertical mixing is responsible for a buoyancy flux F^b, whose bottom boundary condition is the geothermal buoyancy flux:

$$F^b(z = -H) = \frac{\alpha Q_{\text{geo}}}{C_p} \tag{7}$$

They consider a linearized equation of state, in which the heat equation becomes:

$$\frac{d\rho}{dt} = -F_z^b \tag{8}$$

Assuming the dynamics are steady, *non-Boussinesq*, hydrostatic, β-plane, they obtain (their Eq 1):

OSD
5, 281–325, 2008

$$\rho f u = -p_y \tag{9}$$

$$-\rho f v = -p_x \tag{10}$$

$$p_z = -\rho g \tag{11}$$

$$(u\rho)_x + (v\rho)_y + (w\rho)_z = -F_z^b \tag{12}$$

$$\rho = \rho_\circ(1 - \alpha_\theta\theta + \alpha_S S) \tag{13}$$

wherein α_θ and α_S are the thermal and haline contraction coefficients, respectively, and horizontal mixing has been neglected. The momentum and density equations are then combined to yield the vorticity equation:

$$\rho\beta v = f(F^b + \rho w)_z \tag{14}$$

Then Joyce et al. (1986) integrate the equation between the bottom z_b and a level z_1 where advection and diffusion are assumed to balance. This procedure is somewhat ad hoc; without using this assumption (instead, z_1 is arbitrary below the main thermocline), the same equations lead to:

$$\int_{z_b}^{z_1} \rho\beta v \, \mathrm{d}z = f\left(\underbrace{\overline{\rho} w(z_1)}_{10^{-4}} + \underbrace{\rho' w(z_1)}_{10^{-8}} + \underbrace{F^b(z_1)}_{10^{-8}} - \underbrace{F^b(z_b)}_{10^{-8}}\right) \tag{15}$$

where we have used the following values for the calculation of the orders of magnitude

OSD
5, 281–325, 2008

given above:

$$\begin{array}{rll} \alpha_\theta & = 2.10^{-4} & \mathrm{K}^{-1} \\ C_p & = 4.10^{3} & \mathrm{JK}^{-1}\mathrm{kg}^{-1} \\ w & \sim 2.10^{-7} & \mathrm{ms}^{-1} \\ \rho_\circ & = 10^{3} & \mathrm{kgm}^{-3} \\ \rho' & \sim 10^{-1} & \mathrm{kgm}^{-3} \\ F^b(z_1) \sim F^b(z_b) = -\frac{\alpha_\theta}{C_p} Q_{\mathrm{geo}} & \sim 10^{-8} & \mathrm{kgm}^{-2}\mathrm{s}^{-1} \\ Q_{\mathrm{geo}} & \sim 10^{-1} & \mathrm{Wm}^{-2} \end{array} \tag{16}$$

It seems odd to neglect $\rho' w(z_1)+F^b(z_1)$ (advection of temperature anomalies minus downward diffusion) at this level, and to keep only the first and last term, as done in Joyce et al. (1986). While such a balance may exist locally, consistency would commend, in contrast, to neglect the last three terms in front of the first. What this scaling analysis actually reveals is that, to lowest order, thermal perturbations to the density field – whether diffusive or geothermal – do not *directly* affect the vorticity balance. We insist on the difference with the conclusion of Joyce et al. (1986): "*Thus, to lowest order, a geothermal heat flux into the ocean of 50 mW m^{-2}, [...], does not significantly affect the vorticity balance of the abyssal circulation*". Indeed, the remaining vorticity equation is the classical Sverdrup balance (Sverdrup, 1947):

$$\beta v = f w_z \tag{17}$$

While vertical diffusion does not appear *explicitly* in this balance, it does appear in hidden form via w_z. Indeed, the heat equation requires downward turbulent heat flux from the main thermocline to be balanced by an upwelling of cold water from below (Pedlosky, 1996). Similarly, geothermal heating generates a thermally direct circulation that only enters the abyssal vorticity balance via the heat equation.

This suggests that the argument of Joyce et al., which is regarded by many oceanographers as a definitive proof of the dynamical insignificance of geothermal heating,

should be revised. Since it has been shown in Sect. 2.1 that geothermal heating is equivalent to a diapycnal mixing rate of about $1\,cm^2\,s^{-1}$ near the bottom, one cannot neglect geothermal heating without neglecting thermal diffusion. Both fluxes enter the Sverdrup relation indirectly, yet play a crucial role in it[2].

3 Geothermal heating and diapycnal fluxes: the thermodynamic method

3.1 The formation/consumption cycle of bottom water

A fertile view of the thermohaline circulation is that of a cycle of formation, transformation and consumption of water masses. Bottom and deep waters are formed at high latitudes through buoyancy loss to the atmosphere. These physical properties are then "convectively churned" towards great depth (Send and Marshall, 1995), where they are further transformed by processes such as entrainment and sill mixing. Thus isolated from the surface – and remembering that the deep ocean is essentially aphotic below 100 m depth – the only process that can alter these water mass properties is diapycnal mixing, without which the ocean would fill up with cold, dense waters in a few thousand years (Munk, 1966). Hence, in steay-state, forming a water mass is only synonym of circulation if it is consumed. Diapycnal fluxes in the ocean interior, primarily associated with mixing, are then "the return limb of the ocean thermohaline circulation" (Toole et al., 1994), and control the intensity of the AABW circulation (Bryan, 1987). In the introduction of this paper, we have already mentioned a point of primary importance: that geothermal heat flux is systematically positive, thus supplying buoyancy to bottom water. Moreover, its action is precisely limited to bottom water, i.e. an endpoint of the T-S diagram, which means that geothermal heating tends to transform the densest water masses into warmer, lighter water, much like air-sea fluxes transform surface waters.

[2]A more appropriate framework for this analysis would have been the potential vorticity equation in isentropic coordinates (e.g. Eq. 4.37, page 110, in Holton (2004)), which circumvents the rather problematic linearization of the equation of state made in (11).

Indeed, a parcel of Antarctic Bottom Water (AABW) experiences a steady warming while heading North in the vicinity of the seafloor, in the same fashion as air-sea fluxes determine the thermal history of North Atlantic surface water while it ascends to high Northern latitudes (Walin, 1982; Speer and Tziperman, 1992; Large and Nurser, 2001; Marshall et al., 1998; Nurser et al., 1999; Iudicone et al., 2008c). To observe this analogy, one just needs to conceptually flip the ocean upside down, as done in Fig. 5. We can therefore assess the transformation due to geothermal heating following the pioneering concepts developed by Walin (1982) and followers.

3.2 The transformation framework

We shall now consider the ocean in the isopycnal/diapycnal coordinates, which are less intuitive, but are more physically meaningful than the traditional horizontal/vertical coordinates. Geothermal heating is responsible for a buoyancy flux $\mathfrak{B}$:

$$\mathfrak{B}(x,y) = -\frac{\alpha}{C_p} Q_{\text{geo}}(x,y) \tag{18}$$

On the time scales relative to ocean circulation, geothermal heating is assumed to be constant so that $Q_{\text{geo}}(x,y)$ is such as described in Sect. 1. It defines a two dimensional, stationary buoyancy flux, which can then be converted into a transformation per density class $F(\sigma)$ (more precisely σ_4, referenced at 4000 m) using the same formulation as Speer et al. (2000):

$$F(\sigma) = \iint_{\mathbb{A}} \mathfrak{B}(x,y)\delta\left(\sigma'(x,y) - \sigma\right) \mathrm{d}x\mathrm{d}y \tag{19}$$

where $\mathbb{A}$ is the area of the seafloor. The delta function allows to sample the points of the seafloor where the density anomaly $\sigma(x,y)$ equals σ, so that we obtain the integral of the buoyancy flux over a portion of the seabed covered by density classes between, say, σ and $\sigma+\Delta\sigma$. $\Delta\sigma$ is called the binning interval, 0.02 kg m^{-3} in our case. This

probably overestimates the accuracy of our knowledge of the density field at depth, but allows for a numerically more stable solution. The set of possible values for σ is [45.6, 46.2]. $F(\sigma)$ is called the *transformation* by geothermal heat flux, and its derivative with respect to σ the *formation*, denoted by M (Speer and Tziperman, 1992; Nurser et al., 1999).

Define the net advective diapycnal flux $A(\sigma)$ and the diffusive diapycnal flux $D(\sigma)$ by their integral along the isopycnal surface intersecting the bottom (but not the surface; this requires the outcropping zone of AABW to be excluded from the domain):

$$A(\sigma) = \int_{\mathbb{A}_\sigma} \mathbf{u} \cdot \mathbf{n} \, \mathrm{d}S \tag{20}$$

where $\mathbf{n}$ is the unit normal vector to isopycnal σ, $\mathbf{u}$ is the velocity, and dS the surface element of the total area of the isopycnal, $\mathbb{A}_\sigma$. The diffusive flux across isopycnal σ is:

$$D(\sigma) = -\int_{\mathbb{A}_\sigma} \kappa \frac{\partial \sigma}{\partial n} \mathbf{n} \, \mathrm{d}S \tag{21}$$

One can s how (Walin, 1982; Speer et al., 2000; Iudicone et al., 2008c) that mass and density conservation then lead to the transformation equation:

$$F(\sigma) - A(\sigma) - \frac{\partial D}{\partial \sigma} = 0 \tag{22}$$

and the water mass formation equation:

$$M(\sigma) = -\frac{\partial F}{\partial \sigma} + \frac{\partial^2 D}{\partial \sigma^2} = \psi_c \text{ (in steady state)} \tag{23}$$

where ψ_c is the streamfunction at the edge of the domain.

These expressions describe the relationship between the transformation due to bottom buoyancy flux (geothermal), diapycnal advection and diapycnal mixing. The magnitude of F for each density class gives the amount of cross-isopycnal transport required to close the budget, *in the absence of mixing*. With this tool in hand, we can now diagnose the tranformation due to geothermal heating in the ocean.

3.3 Results – impact of a realistic heatflow

In Fig. 6a we present the aforementioned transformation as a function of the density anomaly σ_4 (referenced at 4000 m). The latter was computed using in situ Levitus (1998) potential temperature and salinity data, using the Jackett and McDougall (1995) equation of state. The chosen domain excludes the outcropping zones of the deepest isopycnals (i.e. the Nordic seas and the southernmost part of the Southern Ocean (poleward of 50° S) so that the previous formulae do not need to explicitly include the effect of air-sea fluxes. The resolution at depth is quite problematic in these datasets, as the bottom boundary layer is not resolved. As a consequence, the quantity we compute is not the heat input over the seafloor area delineated by two isopycnals, but rather, the heat released into the bottom layer at some height above the isopycnal intersection with the seafloor.

Figure 6b displays the area represented by each isopycnal on the seafloor (i.e. between two adjacent isopycnals). Figure 6c shows the mean geothermal heat flux by isopycnal. Not surprisingly, the curve is flat in the uniform case whereas the spatially variable heat flux shows a maximum contribution for intermediate densities (σ=45.80), and a minimum for higher densities ($\sigma \simeq 46.00$): the flux is higher in the NADW depth range and decreases on abyssal plains, where the heavier AABW is found. The transformation induced by the spatially uniform heatflow in Fig. 6a has a maximum at σ=45.85, of about 6.5 Sv. This is a bit larger than the transport estimated in Sect. 2.2, but nonetheless surprisingly consistent with this crude estimate. The spatially variable heatflow (Fig. 6c) injects more heat into the intermediate density classes (lighter than σ=45.85) which tends to shift the transformation towards the left(Fig. 6a) , as well as reducing it slightly to 6 Sv. Overall, the difference with a uniform heatflow is fairly small.

Thus, with the current thermohaline structure, this diagnosis reveals that geothermal heating transforms about 6 Sv across the σ=45.90 isopycnal, where we should therefore expect the maximum transport. Moreover, we can also expect spatial variations of the heat flux to shift this transport towards lighter isopycnals. Equation (23) shows

OSD
5, 281–325, 2008

how the convergence of diffusive fluxes prevents the entirety of this transformation to be converted into circulation ψ_c. Typically, turbulent mixing reduces such transports by roughly a factor of two in the surface ocean. This ratio cannot be determined within this thermodynamic framework, so we now turn to a dynamical model to explore the interplay between these two processes.

4 Geothermal heating and the abyssal circulation: the dynamic method

4.1 The OPA model

We employ the OPA ocean GCM (Madec et al., 1998; Delecluse and Madec, 1999), in its global configuration ORCA2-LIM (Timmermann et al., 2005). The horizontal mesh is based on a 2° by 2° Mercator grid (i.e. same zonal and meridional grid spacing) which has been modified poleward of 20° N in order to include two numerical inland poles (Murray, 1996). This modification is semi-analytical (Madec and Imbard, 1996) and based on a series of embedded ellipses. It insures that the mesh remains close to isotropy and that the smallest grid cell is along Antarctica. In order to refine the meridional resolution up to 0.5° at the equator, additional local transformations were applied within the Tropics. There are 31 levels in the vertical, with the highest resolution (10 m) in the upper 150 m. The bottom topography and the coastlines are derived from a global atlas (Smith and Sandwell, 1997). The vertical mixing parameterization scheme is computed by a model based on a turbulent kinetic energy prognostic equation (Blanke and Delecluse, 1993), and there is a diffusive bottom boundary layer parameterization (Beckmann and Doescher, 1997). Vertical mixing asymptotes to a background diffusivity of 0.1 $cm^2\,s^1$ in the deep ocean interior. Mixing due to convection was parameterized by locally enhancing the vertical diffusivity in statically unstable situations. Lateral mixing is computed along isopycnal surfaces, supplemented with the Gent and McWilliams (1990) eddy-induced velocity parameterization (Lazar et al., 1999). The mixing coefficient of the latter depends on the baroclinic instability growth

rate (Treguier et al., 1997). The upper boundary of the model is a linear free surface (Roullet and Madec, 2000).

We ran three sets of experiments, described as follows:

- *CBW experiments*: Preliminary experiments were carried out with a cruder version of the GCM (ORCA2), without a sea ice model. Sea ice cover was prescribed from climatological observations, which tended to produce anomalously cold bottom water (CBW) with very little circulation. Imperfect though it is, this configuration turns out to be very close to the limit case of a homogeneously cold abyssal ocean (cf. Sect. 3), and is therefore useful in understanding the physics of the response to a uniform geothermal heating of 86.4 mW m^{-2} (experiment CBW_Quni).

- *STD experiments*: The reference version of ORCA2-LIM, as decribed above, was used for 3 experiments. The first one has no geothermal heating (experiment STD). The second one differs only by a uniform geothermal heating of 86.4 mW m^{-2} (experiment STD_Quni). The third has the realistic geothermal heatflow of Fig. 1) with the same global mean (experiment STD_Qvar).

- *MIX experiments*: Because the vertical diffusivity of the model is quite low compared to most OGCMs, we performed two additional experiments with ORCA2-LIM with enhanced vertical mixing. The model background vertical diffusivity increases from surface to bottom, mimicking the effects of decreased stratification and increased small-scale turbulence near the bottom. (Values range from 0.12 cm^2 s^{-1} in the first 1000 m to 1.2 cm^2 s^{-1} at 5000 m). Further detail on these experiments can be found in (Iudicone et al., 2008a,b). The first experiments, MIX, is identical to STD except for this modified K_z profile. Similarly, MIX_Qvar is the counterpart of STD_Qvar with enhanced vertical mixing. The setup is summarized in Table 2.

All experiments were carried out to equilibrium ($|\partial_t T| \leq 0.01$ deg / century i.e. ~1500 years). In all the following, the streamfunction is computed on the zonal mean *effec-*

tive velocity; that is, the sum of the Eulerian velocity and the eddy-induced velocity produced by the Gent and McWilliams (1990) parameterization.

4.2 Effect of a uniform geothermal heating

In Fig. 7 we present the results of the CBW set of experiments. The reference experiment, CBW (Fig. 7a) has a fairly weak thermohaline circulation in the North Atlantic Deep Water (NADW) depth range (1000 to 2500 m), partly because of the low vertical mixing rate (0.1 $cm^2\,s^{-1}$). The bottom water circulation is almost non-existent, due to anomalous fluxes resulting from the absence of a realistic sea-ice model, which filled the last 2000 m of the world ocean with anomalously cold water. Together with the low mixing, this strongly inhibits Antarctic Bottom Water (AABW) formation.

Under the influence of a uniform heatflow of 86.4 $mW\,m^{-2}$, the model reacts by producing a fairly intense circulation cell in the AABW depth range: Fig. 7b shows that after 2000 years of integration, the streamfunction difference between experiments CBW and CBW_Quni culminates at ~5 Sv at a depth of 3500 m and 35° S, a fairly significant circulation at this depth.

This transport anomaly is accompanied by a large warming of the abyss, visible in Fig. 7c. The last 3000 m of the model have warmed by 0.1 to 0.5°C, a very large change for this relatively uneventful portion of the ocean. The maximum of 0.5°C at 50° N is located at the bottom of the North Pacific basin. This should not come as a surprise, since we have found in Sect. 2.1 that it is the location where geothermal heating should be felt most strongly (it is equivalent to a diapycnal mixing of ~3 $cm^2\,s^{-1}$ there). In addition, the region exhibits a marked horizontal recirculation in the interior (not shown), allowing bottom water to feel the influence of geothermal heating for a long time. The combined effect of these thermal and kinematic changes is an increase in poleward heat transport by 10% at 50° S (Fig. 12).

The experiments STD and STD_Quni give us complementary information about the adjustment to geothermal heating. The medium panel of Fig. 8 shows the circulation in experiment STD. In contrast to CBW, the presence of an interactive sea-ice leads to

OSD
5, 281–325, 2008

a stronger AABW circulation (6 Sv), resulting in a more realistic thermal structure (not shown). The corresponding case, with uniform geothermal heating is shown in Fig. 9a. As expected from the scaling law (6), the difference is less extreme than for CBW_Quni – CBW, i.e. 3 Sv instead of 5 Sv (an identical Q_{geo} and stronger abyssal temperature gradients in STD_Quni lower the ratio $Q_{geo}/\Delta T$).

In Table 1 we summarize the results obtained by the three independent methods (simple scaling law, thermodynamic method, GCM transport) to evaluate the response of the ocean to a uniform heatflow. The correspondence proves quite good, and works best for the Pacific Ocean, where geothermal heating is likely to have the greater impact (cf. Sect. 2.1). The maximum in transformation is systematically greater than the circulation implied by other methods, implying that diapycnal mixing partially compensates geothermally-induced advection in the model. This occurs because the bottom boundary heatflow acts to erode the initial stratification, which diminishes the downward turbulent heat flux. There is thus less need for a cold water source, which in steady-state implies a circulation slowdown. Therefore, any finite amount of diapycnal mixing will lead to circulations systematically lower than those diagnosed from the geothermal transformation alone. However, the interplay between the two processes is quite non-linear, as will be seen in Sect. 4.4.

4.3 Effect of a spatially variable geothermal heat flux

In Fig. 9c we plot the global streamfunction difference between experiments STD_Qvar and STD_Quni. One can see that the effect of the spatial variations is to reduce the AABW circulation by ∼1.5 Sv (Fig. 9b). In the temperature field (Fig. 10), the effect is to enhance the warming at mid-depth by about 0.02 degrees, and to reduce it near the bottom (by up to 0.1°C in the North Pacific).

This can be easily understood by considering the horizontally-integrated heatflow at each depth in the "realistic" and "uniform" case (Fig. 11). The dash-dotted line, representing the difference between the two cases, explains this result: with a spatially variable heatflow, the ocean receives more heat at moderate depths (2000 to 3000 m)

where the flux is at a maximum near mid-ocean ridges. It receives comparatively less heat below 4000–4500 m, where the realistic heatflow falls under its global average (~50 mW m^{-2} vs. 86.4 mW m^{-2}). Because heat is now deposited at shallower levels, the temperature field follows suit. The consequence is that maintaining the abyssal temperature heat balance in STD_Qvar can be achieved with a weaker AABW circulation than in STD_Quni, as observed in Fig. 9b.

4.4 Effect of vertical mixing

Some of the preceding results are arguably a consequence of the low vertical mixing rate used in the model (K_z), which does not take into account the increase in near-bottom mixing rate shown by observational studies (e.g. Toole et al., 1994). We wish to know whether our results stand in the case of a more realistic K_z profile, which would modify the deep thermohaline structure upon which geothermal heating is acting, in a fundamentally non-linear manner. Experiment MIX has a vertical mixing rate increasing from 0.12 cm^2 s^{-1} in the thermocline to 1.2 cm^2 s^{-1} at 5000 m. Based on the work of Bryan (1987) and followers, we expect that this increase will enhance the intensity of the meridional overturning circulation (MOC) and this is indeed what is observed (Fig. 8b, c, and d): between experiments STD and MIX, the NADW circulation increases from 14 to 16 Sv, the AABW circulation from 6 to 12 Sv. This is a more reasonable estimate owing to the water-mass analyses of Orsi et al. (1999) and Ganachaud and Wunsch (2000).

The corollary effect is that horizontal surface temperature gradients (primarily meridional, on very large scales) are mapped by vertical diffusion onto the near bottom temperature field, which thus becomes less homogenous than in the limit of no vertical mixing (experiments CBW). Hence our scaling law (Eq. 6) predicts a smaller geothermal circulation to keep the deep ocean in thermal equilibrium, as a consequence of the low ratio $Q_{geo}/\Delta T$.

Since we have already seen the effect of a realistic geothermal heating on the model in the previous section, we ran only one experiment with non-zero geothermal flow, one

where it is spatially varying (MIX_Qvar). The difference (MIX_Qvar− MIX) is presented in Fig. 9. The general bottom circulation is otherwise very similar. Figure 9 shows a maximum of 1.5 Sv for the geothermal circulation, which is about 10% of the total AABW circulation in MIX_Qvar.

Thus, we find that for a strong abyssal mixing rate, the dynamical effect of a realistic heatflow is to enhance the AABW circulation by 1.5 Sv, weaker than in STD_Qvar. The thermodynamic effect is also reduced: a large-scale warming of abyssal oceans by about 0.15°C peaking around 0.3°C in the bottom North Pacific (not shown).

Therefore, the interaction of geothermal heating and diapycnal mixing is quite nonlinear. As explained above, this is because both forcings critically affect the deep stratification, which conditions both the strength of the downward diffusive heat flux and the intensity of the geothermal circulation.

4.5 Effect on heat transport

In Fig. 12 we show how geothermal enhances poleward heat transport in the Southern Hemisphere (and very modestly so in the Northern Hemisphere). The reason is that the additional, geothermal heat input of 0.03 PW must be evacuated from the abyss, which is achieved by warming AABW and enhancing its circulation.

It is remarkable that experiments with such different thermal structures and circulations as CBW and MIX end up displaying very similar changes in heat transport (∼10% increase in poleward heat transport in both cases). Whether the flux is uniform or realistic seems to induce almost no difference in transport at all (STD experiments, not shown). The changes between CBW and MIX are, however, not identical in the Southern Ocean, where most of the heat is released to the atmosphere. In CBW, where the background circulation is so weak and stratification so strong, geothermal heating produces a maximum transport anomaly near 50° S, peaking at −0.07 PW (about twice the geothermal forcing). In the MIX experiments, the model reacts much more moderately to the addition of the forcing, peaking at −0.04 PW. This is another illustration of the nonlinear interplay between geothermal heating and diapycnal mixing.

5 Discussion

We have explored the dynamical role of geothermal heating in the abyssal circulation using three different and largely independent approaches. These led us to the following conclusions:

- Geothermal heating can force a circulation in the abyss, comparable to the Stommel-Arons circulation. This forcing enhances the Antarctic Bottom Water overturning cell by about 1.5 to 5 Sv in our GCM experiments, consistent with simple scaling arguments and a density-binning diagnosis. The low end of this range is smaller than the error bar of the current estimates of AABW circulation, therefore the dynamical effect can overall be considered weak: it is not a first order feature, but not a negligible one either.

- On the other hand, the thermodynamic response is considerable, with bottom waters warming by about 0.3°C, with a maximum of 0.5°C in the North Pacific bottom waters, in agreement with Adcroft et al. (2001). This is an enormous contribution to the heat budget of the deep ocean, and should no longer be neglected.

- Geothermal heat flux is formally analogous to air-sea fluxes, and likewise, it induces a transformation of water masses (AABW in this case). However, an essential distinction is to be made: geothermal heating does not form any water mass stricto sensu, and rather, its systematically positive sign leads to consume the densest water masses.

- In that sense, it is directly analogous to diapycnal mixing, both qualitatively and quantitatively. It has a similar effect on bottom water, eroding extrema of the global T-S diagram and depositing a comparable amount of heat in the abyss. On a global scale, it is in fact equivalent to a diapycnal mixing coefficient of $\sim 1.2\,\mathrm{cm^2\,s^{-1}}$ at 3500 m, i.e. the canonical value of (Munk, 1966). In regions of weak deep stratification (e.g. North Pacific) where downward diffusive fluxes are

OSD
5, 281–325, 2008

small, it should therefore prevail in the dynamics and thermal structure, which is confirmed by GCM experiments.

- The density-binning method allows to quantify the water-mass transformation induced by geothermal heat flux. Best estimates of the spatial variability of the flux and of the deep thermohaline structure yield a transformation maximum of ~6 Sv at σ_4=45.90 (in the AABW range). This rate can be thought of as the *expected circulation in the absence of mixing*; in the presence of mixing it will be partially compensated by the divergence of diffusive fluxes.

- Indeed, any amount of diapycnal mixing will lead to circulations systematically lower than diagnosed from geothermal transformation alone. The interplay between the two processes is quite non-linear, with geothermal heating reducing the deep thermal stratification upon which diffusion is acting, while vertical mixing alters the lateral temperature gradients that support a geothermal circulation.

- The spatial structure of the flux yields, consistently with its vertical distribution, a weaker response at great depth (abyssal plains) than in the uniform case. The relative cooling reaches up to 0.06–0.08°C there, with an opposite response at the typical depth of mid-ocean ridges (2500 m), which warm up by about 0.02°C. The mean overturning circulation is then reduced by ~0.5 to 1 Sv. The difference is weakened in the case of strong vertical mixing.

- A remarkable finding is that the ocean heat transport was nearly constant in all experiments, despite the wide range of thermal and circulation changes they cover. The presence of a geothermal heatflow, whether spatially variable or not, means that the ocean must evacuate an additional 0.03 PW, which it does in all cases by enhancing poleward heat transport in the Southern Hemisphere, peaking at about 10% near 50° S.

Our numerical results are broadly consistent with Adcroft et al. (2001) and Scott et al. (2001), in that they confirm that the geothermal circulation is inversely proportional

to near-bottom temperature gradients. Also, both studies show a very strong thermodynamic response and a fairly weak dynamical response. This is somewhat surprising: in this mode of heating at low-geopotential heights, the ocean was expected to behave like a heat engine (Huang, 1999; Marchal, 2007), yet we find that most of the heat input goes into raising the potential energy of the ocean. Very little of it is actually converted into kinetic energy. This confirms that heat fluxes are rather inefficient sources of motion in the ocean, compared to momentum fluxes due to winds or tides (Wunsch and Ferrari, 2004). We note, however, that some portion of this potential energy must also serve to achieve mixing, as pointed out by Huang (1999), However, no significant changes in convective instability were noticed here.

The effect of geothermal heat fluxes is largely confined to the heat balance; like diapycnal heat fluxes, it is only a driving force of the circulation via the heat equation. As clearly demonstrated by Scott et al. (2001), this is because advection is the most efficient way of removing heat from the abyss. However, these heat fluxes have no impact, to lowest order, on the vorticity balance, which is perhaps why the induced circulation is weak. There is a fundamental difference, however: diapycnal fluxes act throughout the water column, below the main thermocline. While comparable in magnitude in the deepest layers, geothermal heating acts only on the densest water masses, with very little impact higher in the water column.

In this work as in most studies, we have fixed the mixing coefficient K_z, disregarding the energetic requirements of the mixing process. If, as suggested by Huang (1999), we were to fix the *energy* available for mixing, the turbulent heat flux would then be constrained by the mechanical input from winds and tides (Wunsch and Ferrari, 2004), and geothermal circulation should be presumably less sensitive to the mixing rate. This will be left for future work.

The case is hereby made for geothermal heating as an important actor of abyssal dynamics. We recommend its inclusion in every model dealing with the long-term ocean circulation, for it substantially alters bottom water mass characteristics and generates a non-negligible circulation in the present-day climate. Moreover, we predict its dynam-

ical effect to be larger in a world of weaker diapycnal mixing. This may plausibly have been the case at the Last Glacial Maximum (LGM), because of strong haline stratification of the abyssal ocean (Adkins et al., 2002). In such a case, geothermal heating could have been the driving force preventing stagnation of the abyssal ocean in the face of strong stratification. Finally, and while its quite steady nature over millenial timescales does not make him an obvious candidate for triggering climate change, there is the intriguing possibility that it convectively destabilized the water column under sea-ice cover at some times in the past, thus modifying, for example, the northern North Atlantic ocean circulation of the Little Ice Age, as conjectured by Weyl (1968). A recent study by Adkins et al. (2005) also goes into this direction, which should be pursued in future work.

Acknowledgements. The authors acknowledge funding by the CNRS and the Ecole Normale Suprieure, and are indebted to Jess Adkins for useful comments. Most of the results presented in this paper were obtained during JEG's "stage de DEA" at LOCEAN in 2001, for which Marina Levy, Christophe Menkes, Sebastien Masson and Mathieu Langaigne are warmly thanked.

References

Adcroft, A., Scott, J. R., and Marotzke, J.: Impact of geothermal heating on the global ocean circulation, Geophys. Res. Let., 29, 1735–1738, 2001. 284, 303, 304

Adkins, J. F., Ingersoll, A. P., and Pasquero, C.: Rapid climate change and conditional instability of the glacial deep ocean from the thermobaric effect and geothermal heating, Quaternary Sci. Rev., 581–594, doi:10.1016/j.quascirev.2004.11.2005, 2005. 306

Adkins, J. F., McIntyre, K., and Schrag, D. P.: The Salinity, Temperature, and δ^{18}O of the Glacial Deep Ocean, Science, 298(5599), 1769, doi:10.1126/science.1076252, 2002. 306

Arakawa, A.: Design of the UCLA general circulation model. Numerical simulation of weather and climate, Tech. Rep. 7, Dept. of Meteorology, University of California, Los Angeles, 116 pp., 1972.

Arhan, M., Mercier, H., Bourles, B., and Gouriou, Y.: Hydrographic sections across the Atlantic at 7 degrees 30N and 4 degrees 30S, Deep Sea Res. I, 45(6), 829–872, 1998. 283

Beckmann, A. and Doescher, R.: A method for improved representation of dense water spreading over topography in geopotential-coordinate models, J. Phys. Oceanogr., 27, 581–591, 1997. 297

Blanke, B. and Delecluse, P.: Variability of the tropical Atlantic Ocean simulated by a general circulation model with two different mixed-layer physics, J. Phys. Oceanogr., 23, 1363–1388, 1993. 297

Bryan, K.: Parameter sensitivity of primitive equation ocean general circulation models, J. Phys. Oceanogr., 17, 970–985, 1987 288, 293, 301

Delecluse, P. and Madec, G.: Ocean modelling and the role of the ocean in the climate system, in: Modeling the Earth's Climate and its Variability, Les Houches, Session LXVII 1997, edited by: Holland, W. R., Joussaume, S., and David, F., Elsevier Science, 237–313, 1999. 297

ETOPO5: Global $5' \times 5'$ depth and elevation (available from National Geographic Data Center, NOAA, US Department of Commerce, Code E/GC3, Boulder, CO 80303), 1986.

Fekece, B. M, Vorosmarty, C. J., and Grabs, W.: Global, composite runoff fields based on observed river discharge and simulated water balances, Tech. Rep., GRDC, 115 pp., 2000.

Ganachaud, A. and Wunsch, C.: Improved estimates of global ocean circulation, heat transport and mixing from hydrographic data, Nature, 408, 453–457, doi:10.1038/35044048, 2000. 301

Gent, P. and Mc Williams, J.: Isopycnal mixing in ocean circulation models, J. Phys. Oceanogr., 20, 105–155, 1990. 297, 299

Gordon, A. L. and Gerard, R. D.: North Pacific bottom potential temperature. in: Geological Investigations of the North Pacific, edited by: Hays, J. D., GSA Memoir 126, 23–39, 1970. 290

Gregg, M. C.: Scaling turbulent dissipation in the thermocline, J. Geophys. Res. Oceans, 94(C7), 9686–9698 , 1989. 287

Guilyardi, E.: Rôle de la physique océanique sur la formation/consommation des masses d'eau dans un modèle couplé océan-atmosphère, PhD Thesis, Université Pierre et Marie Curie, Paris, France, 1997.

Guilyardi, E., Madec, G., and Terray, L.: The role of lateral ocean physics in the upper ocean thermal balance of a coupled ocean-atmosphere GCM, Clim. Dynam., 17, 589–599, 2001.

Holton, J. R.: An Introduction to Dynamic Meteorology, 4th Ed., Elsevier, 535 pp., ISBN 012354016X, 2004. 293

Huang, R.: Mixing and energetics of the thermohaline circulation, J. Phys. Ocean., 29(4) 727–

746, 1999. 283, 284, 305
Iudicone, D., Speich, S., Madec, G., and Blanke, B.: The global conveyor belt from a Southern Ocean perspective, J. Phys. Oceanogr., in press, 2008a. 288, 298
Iudicone, D., Madec, G., Blanke, B., and Speich, S.: The role of Southern Ocean surface forcings and mixing in the global conveyor, J. Phys. Oceanogr., in press, 2008b. 288, 298
Iudicone, D., Madec, G., and McDougall, T. J.: Watermass transformations in a neutral density framework and the key role of light penetration, J. Phys. Oceanogr., in press, 2008c. 294, 295
Jackett, D. R. and McDougall, T. J.: Minimal adjustment of hydrographic data to achieve static stability, J. Atmos. Ocean. Tech., 12, 381–389, 1995. 296
Jouzeau, A.: Paramétrisation du mélange latéral de méso-échelle dans ORCA le modèle de circulation générale océanique, Rapport de stage de DEA de Mécanique des Fluides et Transferts thermiques de l'Ecole centrale de Nantes, 53 pp., 1999.
Joyce, T. M., Warren, B. A., and Talley, L. D.: The geothermal heating of the abyssal subartic pacific ocean, Deep-Sea Res., 33(8), 1003–1015, 1986. 290, 291, 292
Kunze, E. and Sanford, T. B.: Abyssal Mixing: Where It Is Not, J. Phys. Oceanogr., 26, 2286–2296, 1996. 287
Large, W. G. and Nurser, A. J. G.: Ocean surface water mass transformation, in: Ocean Circulation and Climate: Observing and Modelling the Global Ocean, edited by: Siedler, G., Church, J., and Gould, J., International Geophysics Series, Vol. 77, Academic Press, 317–336, 2001. 294
Lazar A., Madec, G., and Delecluse, P.: The Deep Interior Downwelling, the Veronis Effect and Mesoscale Tracer Transport Parameterizations in an OGCM, J. Phys. Oceanogr., 29, 2945–2961, 1999. 297
Levitus, S.: Climatological atlas of the world ocean, Tech. rep., NOAA, Rockville, Md., 1998. 282, 286, 296
Ledwell, J. R., Watson, A. J., and Law, C. S.: Mixing of a tracer across the pycnocline, J. Geophys.Res., 103, 21 499–21 529, 1998. 287
Madec, G. and Imbard, M.: A global ocean mesh to overcome the North Pole singularity, Clim. Dyn., 12, 381–388, 1996. 297
Madec, G., Delecluse, P., Imbard, M., and Levy, C.: OPA Version 8.1 Ocean General Circulation Model Reference Manual, Tech. Rep. LODYC/IPSL Note 11, 1998. 297
Marchal, O.: Particle transport in horizontal convection: Implications for the "Sandström theo-

rem", Tellus A, 59(1), 141–154, 2007. 305
Marshall, J. C., Jamous, D., and Nilson, J.: Reconciling 'thermodynamic' and 'dynamic' methods of computation of water mass transformation rates, Deep-Sea Res., 46, 545–572, 1998. 294
Müller, R. D., Roest, W. R., Royer, J.-Y., Gahagan, L.M., and Sclater, J. G.: Digital isochrons of the ocean floor, J. Geophys. Res., 102(32), 3211–3214, 1997. 284, 285
Munk, W.: Abyssal recipes, Deep-Sea Res., 13, 707–730, 1966. 286, 293, 303
Munk, W. and Wunsch, C.: Abyssal recipes II: Energetics of tidal and wind mixing, Deep-Sea Res., 45, 1977–2010, 1998. 286
Murray, R. J.: Explicit generation of orthogonal grids for ocean models, J. Comput. Physics., 126, 251–273, 1996. 297
Nurser, A. J. G., Marsh, R., and Williams, R. G.: Diagnosing water mass formation from air-sea fluxes and surface mixing, J. Phys. Ocean., 29, 1468–1483, 1999. 294, 295
Orsi, A. H., Johnson, G. C., and Bullister, J. L.: Circulation, mixing, and production of Antarctic Bottom Water, Prog. Oceanog., 43(1), 55–109, 1999. 301
Pedlosky, J. P.: Ocean Circulation Theory, Springer-Verlag, 453 pp., 1996 292
Pollack, H. N., Hurter, S. J., and Johnson, J. R.: Heat flow from the Earth's interior: analysis of the global dataset, Rev. Geophys., 31, 3, 276–280, 1993. 284, 285
Polzin, K. L., Toole, J. M., Ledwell, J. R., and Schmitt, W. R.: Spatial variability of turbulent mixing in the abyssal ocean, Science, 276, 93–96, 1997.
Roullet, G. and Madec, G.: Salt conservation, free surface and varying levels: a new formulation for ocean general circulation models, J. Geophys. Res., 105, 23, 927–942, 2000. 298
Send, U. and Marshall, J.: Integral effects of deep convection, J. Phys. Oceanogr., 25, 855–872, 1995. 293
Sclater, J. G.: Ins and outs on the ocean floor, Nature, 421, 590–591, 2003.
Scott, J. R., Marotzke, J., and Adcroft, A.: Geothermal heating and its influence on the meridional overturning circulation, J. Geophys. Res., 106, 1–14, 2001. 284, 289, 290, 304, 305
Smith, W. H. F. and Sandwell, D. T.: Global sea floor topography from satellite altimetry and ship depth sounding, Science, 277, 1956–1962, 1997. 297
Speer, K. and Tziperman, E.: Rates of water mass formation in the North Atlantic ocean, J. Phys. Ocean., 22, 93–104, 1992. 294, 295
Speer, K., Guilyardi, E., and Madec, G.: Southern Ocean transformation with or without eddy mass fluxes, Tellus, 52(5), 544–565, 2000. 294, 295

Stein, A. and Stein, C.: A model for the global variation of depth and heat flow with lithospheric age, Nature, 359, 123–129, 1992. 283, 285, 314
Stommel, H. and Arons, A. B.: On the abyssal circulation of the world ocean- II. An idealized model of circulation pattern and amplitude in oceanic basins, Deep-Sea Res., 6 , 217–233, 1960. 283, 288
Stommel, H., Arons, A. B., and Faller, A. J.: Some examples of stationary planetary flow patterns in bounded basins, Tellus, 10, 179–187, 1958. 283
Sverdrup, H. U.: Wind-driven currents in a baroclinic ocean, with application to the equatorial currents of the eastern Pacific, Proc. Natl. Acad. Sci., 33, 318–326, 1947. 292
Timmermann, R., Goosse, H., Madec, G., Fichefet, T., Ethé, C., and Dulière, V.: On the representation of high latitude processes in ORCA-LIM global coupled sea-ice-ocean model, Ocean Model., 8, 175–201, 2005. 297
Toggweiler, J. R. and Samuels, B.: Effect of Drake passage on the global thermohaline circulation, Deep Sea Res. I, 42(4), 477–500, 1995. 283, 288
Toggweiler, J. R. and Samuels, B.: On the ocean's large-scale circulation near the limit of no vertical mixing, J. Phys. Oceanogr., 28(9), 18320–1852,1998. 283, 288
Toole, J. M., Polzin, K. L., and Schmitt, R. W.: Estimates of diapycnal mixing in the abyssal ocean, Science, 264, 1120–1123, 1994. 293, 301
Treguier, A. M., Held, I. M., and Larichev, V. D.: Parameterization of Quasigeostrophic Eddies in Primitive Equation Ocean Models, J. Phys. Oceanogr., 27, 567–580, 1997. 298
Turcotte, D. and Schubert, G.: Geodynamics. Application of continuum physics to geological problems, John Wiley & Sons, 450 pp., 1982.
Unesco: Algorithms for computation of fundamental properties of sea water, Unesco Tech. Pap. Marine Science 44, Unesco, 1983.
Warren, B. A.: Deep circulation of the world ocean, in: Evolution of physical oceanography, edited by: Warren, B. A. and Wunsch, C., MIT Press, Cambridge, 6–41, 1981. 283
Vine, F. J. and Matthews, D. H.: Magnetic anomalies over oceanic ridges, Nature, 199, 947–951, 1963.
Visbeck, M., Marshall, J., Haine, T., and Spall, M.: Specification of Eddy Transfer Coefficients in Coarse-Resolution Ocean Circulation Models, J. Phys. Oceanogr., 27, 381–402, 1997.
Visbeck, M.: Power of pull, Nature, 447(7143), p. 383, 2007. 283
Walin, G.: On the relation between sea-surface heat flow and thermal circulation in the ocean, Tellus, 34, 187–195, 1982. 282, 294, 295

Webb, D. J. and Suginohara, N.: Vertical mixing in the ocean, Nature, 409, p. 37, 2001. 283, 288

Weyl, P. K.: The Role of the Oceans in Climatic Change: A Theory of the Ice Ages, Meteorological Monographs, 8, 37–62, 1968. 306

Whitworth, T., Warren, B. A., Nowlin, W. D., Rutz, S. B., Pillsbury, R. D., and Moore, M. I.: On the deep western-boundary current in the Southwest Pacific Basin, Prog. Oceanog. 43(1), 1–54, 1999. 283

Wunsch, C. and Ferrari, R.: Vertical Mixing, Energy, and the General Circulation of the Oceans, Ann. Rev. Fluid Mech., 36, 281–314, 2004. 305

Xie, P. and Arkin, P. A.: Analysis of global precipitation using gauge observations, satellite estimates and numerical model predictions, J. Climate, 9, 840–858, 1996.

Table 1. Quantification of the geothermally induced transports using three different methods. The figures in the "Levitus" column refer to the transport calculated using Eq. (2). The "Model" figures are derived from the CBW experiment described in Sect. 4. The transformation (Sect. 3) is calculated in both cases by binning the density field obtained from either Levitus data or model output. The last column is the sum of the numbers of the previous columns for each category.

Basin	Atlantic		Indian		Pacific		Total	
Area (10^{14}m^2)	0.34		0.45		0.99		1.78	
	Levitus	Model	Levitus	Model	Levitus	Model	Levitus	Model
ΔT (°C)	1.90	0.8	0.96	0.86	0.42	0.6	–	–
Transport (Sv)	0.5	1.3	0.8	0.9	5.2	3.7	6.5	5.9
Model Transport (CBW, in Sv)	–	0.5	–	1.	–	3.5	–	5
Max. Transformation (Sv)	–2.1	–	–1.3	–	–5.1	–	–8.5	–

OSD
5, 281–325, 2008

Table 2. Summary of the numerical experiments used in this study. The numbers given for Q_{geo} are its global mean in each experiment.

Set	Experiment	Q_{geo} (mW m^{-2})	K_z (cm^2 s^{-1})
CBW	CBW	Uniform, 0	0.1
	CBW_Quni	Uniform, 86.4	0.1
STD	STD	Uniform, 0	0.1
	STD_Quni	Uniform, 86.4	0.1
	STD_Qvar	Variable, 86.4	0.1
MIX	MIX	Uniform, 0	0.1 to 1.2
	MIX_Qvar	Variable, 86.4	0.1 to 1.2

OSD
5, 281–325, 2008

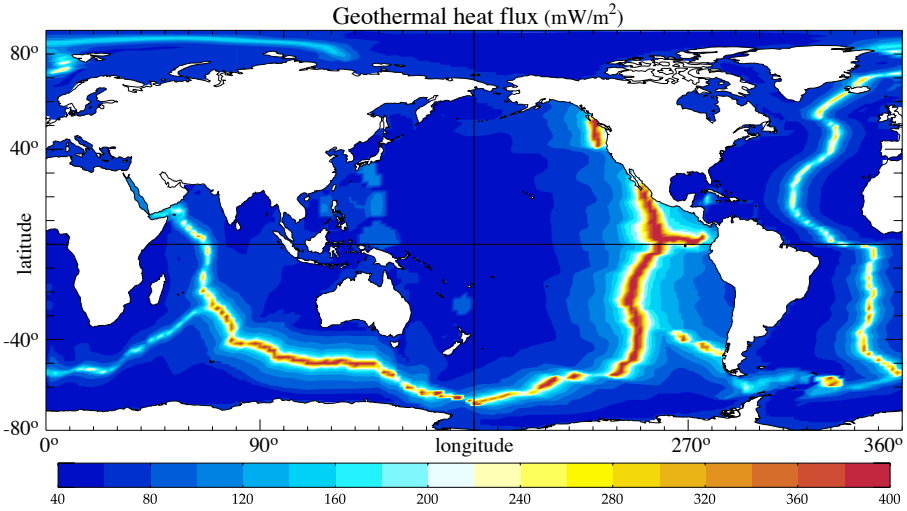

Fig. 1. Geothermal heat flux, as inferred from the age of the seafloor and the formulae of Stein and Stein (1992) (Eq. 1).

OSD
5, 281–325, 2008

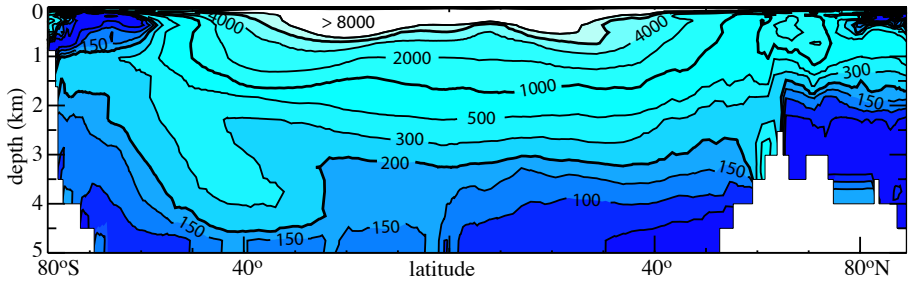

Fig. 2. Downward diffusive heat flux ($K_z \frac{\partial T}{\partial z}$) for a turbulent diffusivity of 1 $cm^2 s^{-1}$. Units: $mW\,m^{-2}$.

OSD
5, 281–325, 2008

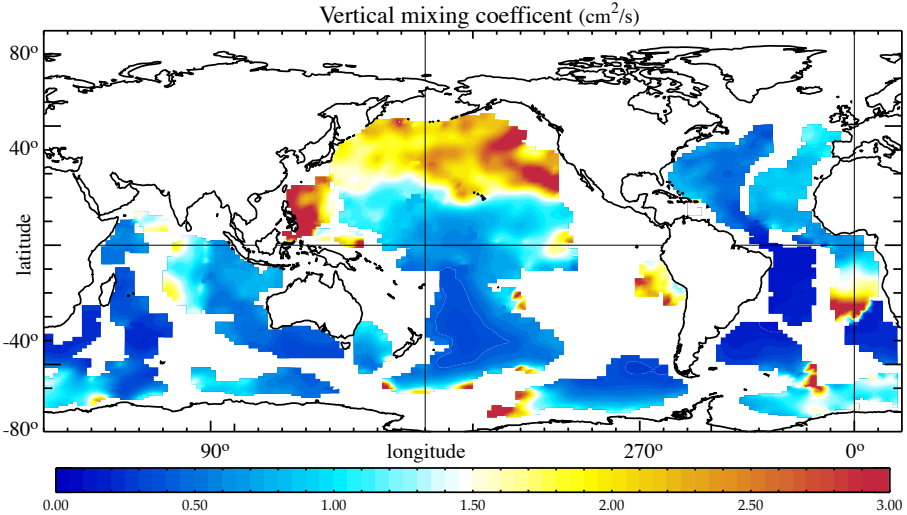

Fig. 3. Equivalent K_z at 4000 m (see text for details). The quantity averages to 1.2 $cm^2\ s^{-1}$.

OSD
5, 281–325, 2008

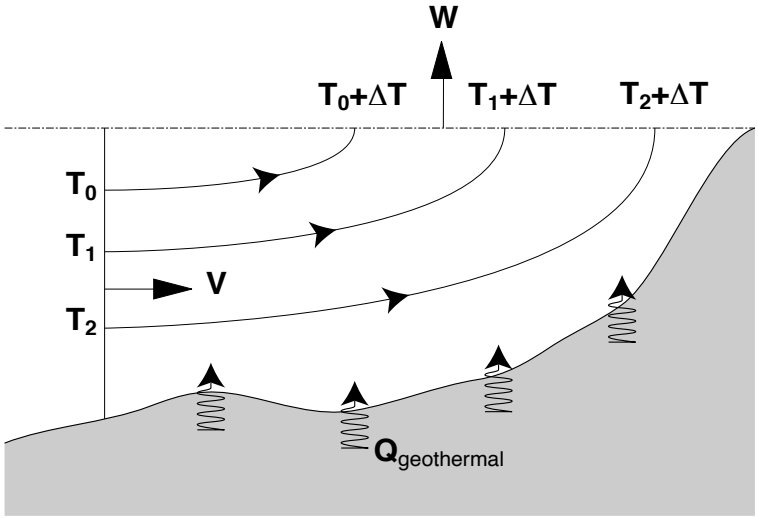

Fig. 4. Schematic of the geothermally-induced circulation. Note that in this formulation, the temperature increase is the same along each streamline (denoted with arrows), which are distinct from isotherms.

OSD
5, 281–325, 2008

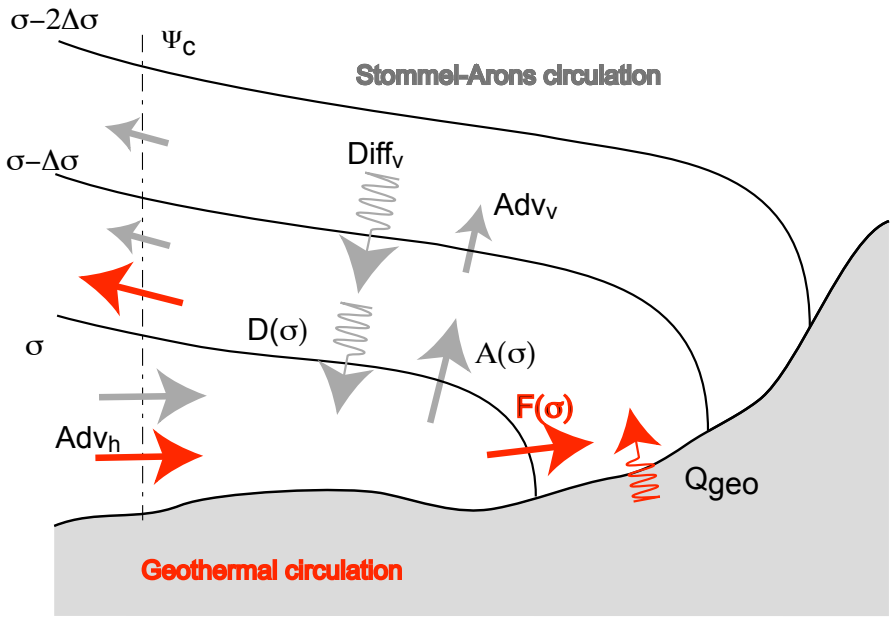

Fig. 5. Transformation of bottom water induced by geothemal heating. See text for details.

OSD
5, 281–325, 2008

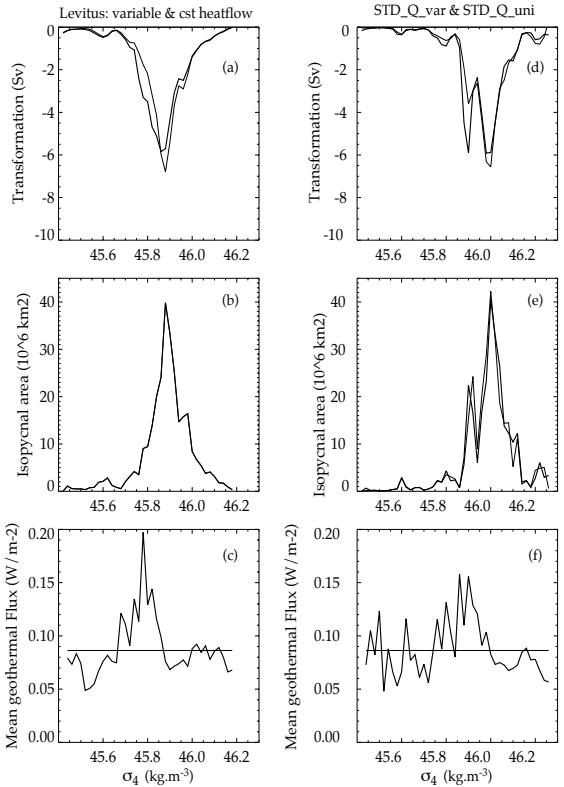

Fig. 6. Density binning in the abyssal ocean. The left hand side shows the result of the density binning method projected onto the thermohaline structure from Levitus. The right hand side refers to numerical experiments STD_Quni and STD_Qvar. **(a)** and **(d)**: transformation for a spatially variable (bold line) and uniform (solid line) heatflow. **(b)** and **(e)**: Area spanned by each pair of isopycnals (with a 0.02 kg m^{-3} binning interval). **(c)** and **(f)** geothermal heat fluxes distribution among isopycnals. The upper curves can be roughly obtained by multiplying the area by the flux in each density bin (i.e. $(a) \simeq (b) \times (c)$ and $(d) \simeq (e) \times (f)$).

OSD
5, 281–325, 2008

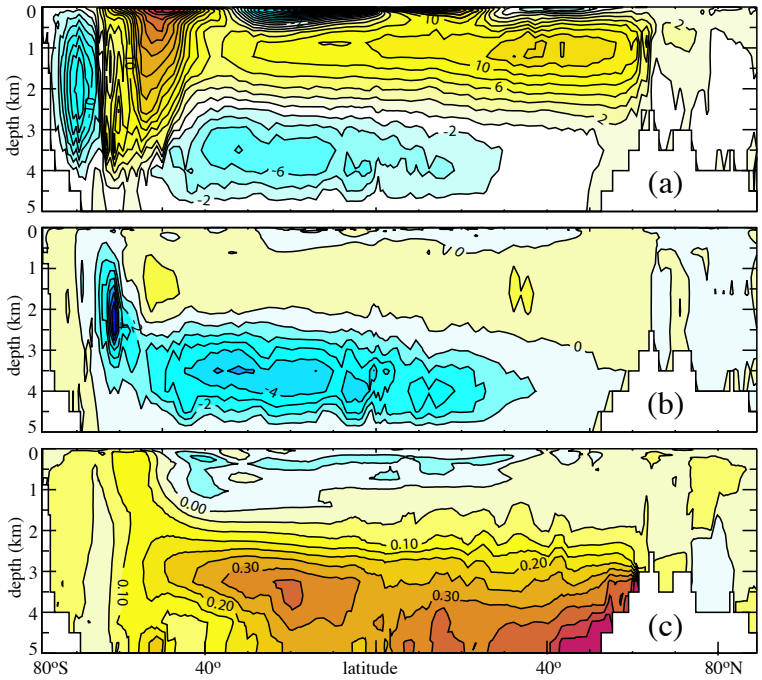

Fig. 7. Outcome of the CBW simulations after 2100 years of integration. **(a)** Meridional effective overturning streamfunction (Ψ_{eff}, Sv) in CBW. **(b)** Ψ_{eff} difference, CBW_Quni – CBW (Sv) **(c)** Potential temperature difference (CBW_Quni – CBW) in ˚C. Note the intensification of the bottom water circulation of about 5 Sv in CBW_Qgeo_uni, and the zonal mean warming of the bottom 2000m of the ocean.

OSD
5, 281–325, 2008

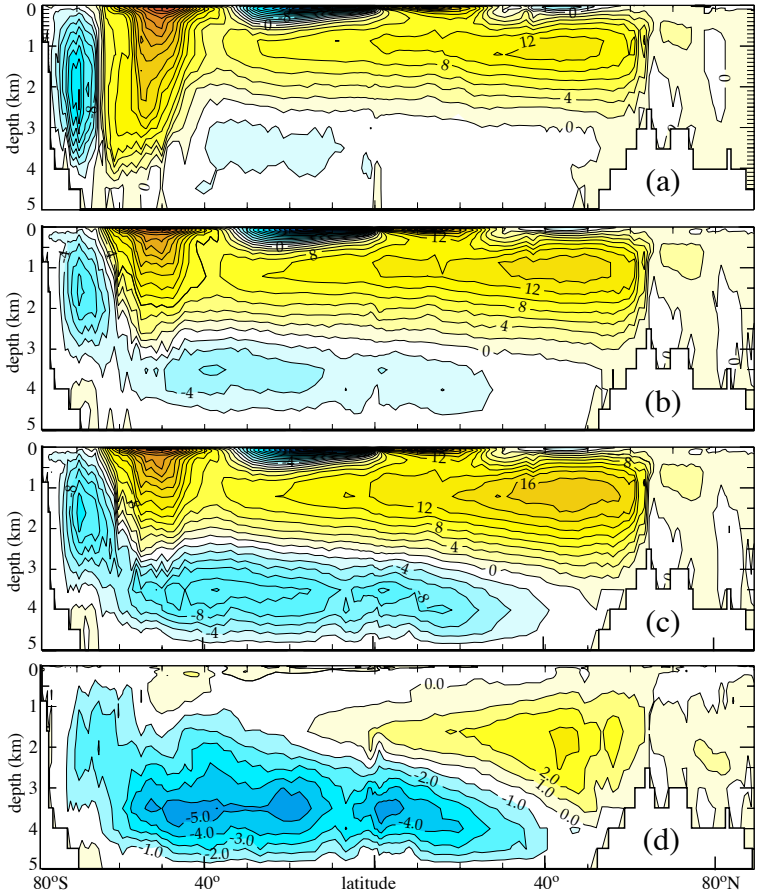

Fig. 8. Global meridional streamfunction (Ψ_{eff}, Sv) for the 3 reference experiments: **(a)** CBW, **(b)** STD, **(c)** MIX and **(d)** $\Delta\Psi_{eff}$: MIX − STD (Sv). Note the large increase in circulation from STD to MIX, particularly for AABW. Note that the contour interval has been decreased from 2 to 0.5 Sv in (d).

OSD
5, 281–325, 2008

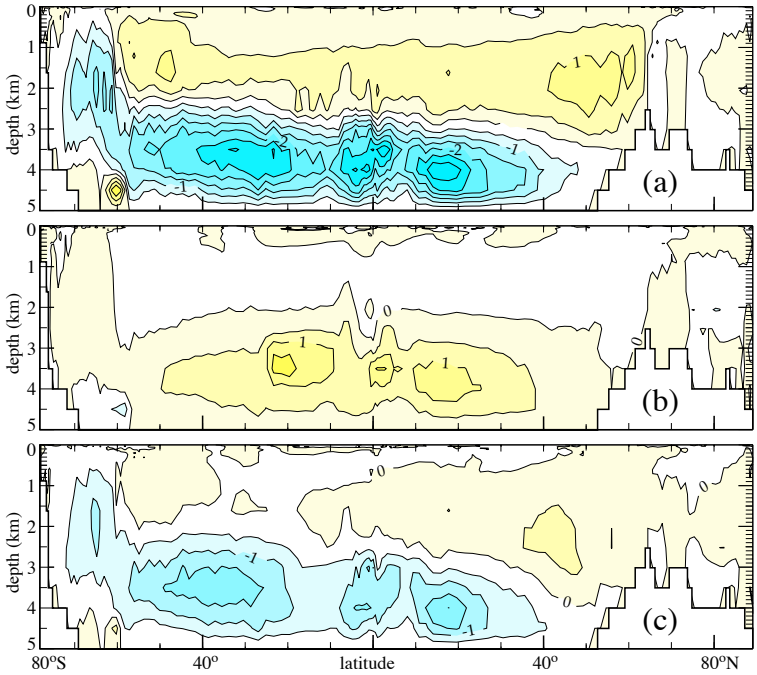

Fig. 9. Global meridional streamfunction difference ($\Delta\Psi_{eff}$, Sv) for 4 doublets of experiments: **(a)** CBW_Quni – CBW; **(b)** STD_Qvar – STD_Quni, **(c)** MIX_Qvar – MIX.

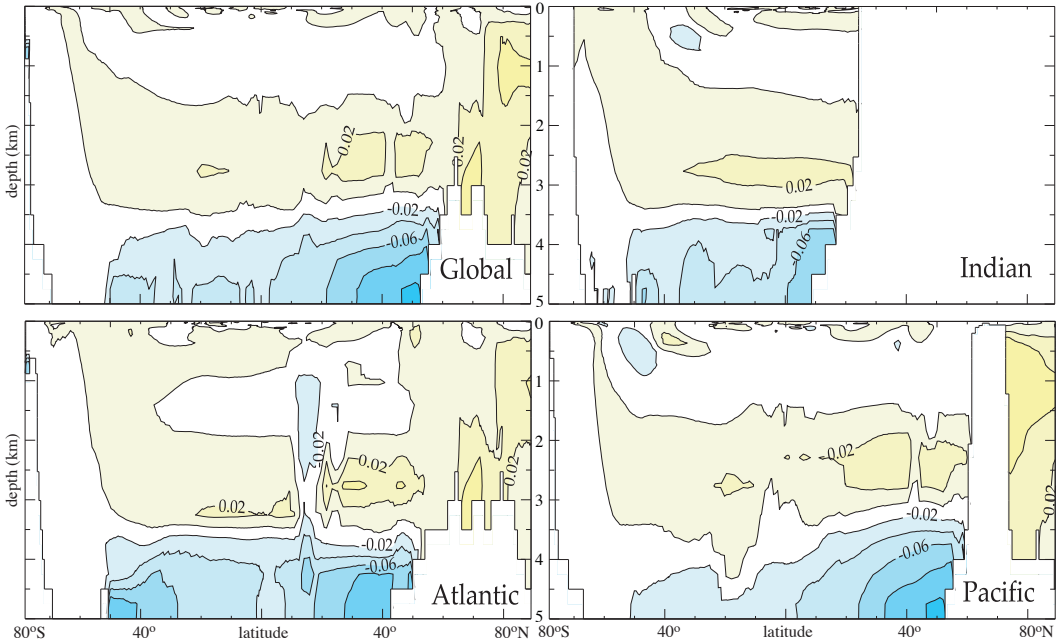

Fig. 10. Potential temperature difference between STD_Qvar and STD_Quni at equilibrium (°C).

OSD
5, 281–325, 2008

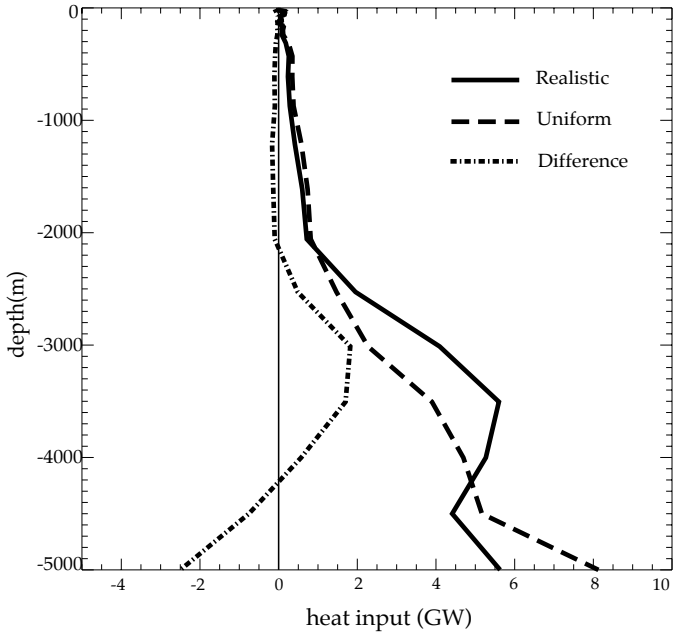

Fig. 11. Vertical distribution of geothermal heating weighted by the seafloor area at each depth. Solid line: realistic spatial structure (cf Fig, 1). Dashed line: uniform heat flow (86.4 mW m^{-2}). Dash-dotted: "realistic" minus "uniform".

OSD
5, 281–325, 2008

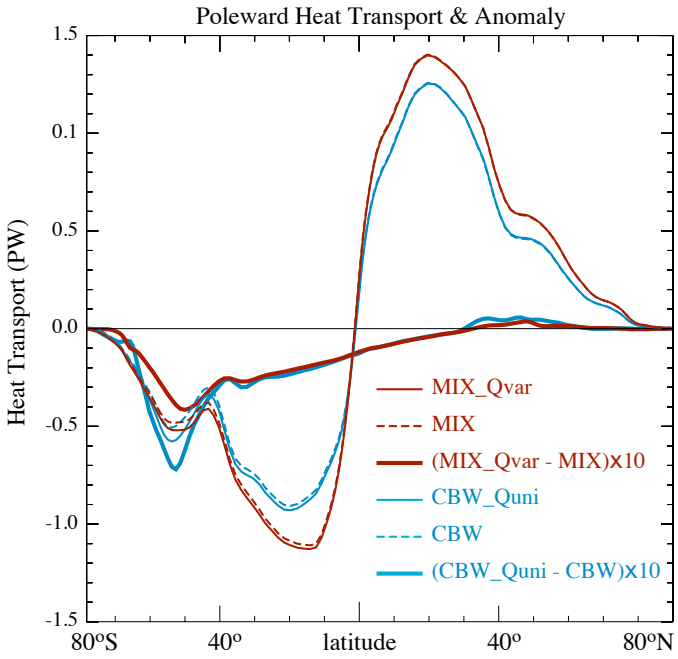

Fig. 12. Global meridional heat transport. Only two extreme cases are presented , from the CBW and MIX families of experiments. Note that the differences (CBW_Quni – CBW) and (MIX_Qvar – MIX) have been multiplied by 10: the additional heat transport due to geothermal heating peaks at about 10% of the total around 50° S.

OSD
5, 281–325, 2008